

Simulation of the Effect of Improved Ground Clocks on GPS Timing Performance

Matthias Suess⁽¹⁾ and Demetrios Matsakis⁽²⁾

⁽¹⁾German Aerospace Centre (DLR)
Oberpfaffenhofen, Germany

⁽²⁾United States Naval Observatory (USNO),
Washington, D.C., USA

BIOGRAPHY

Matthias Suess studied Computer Science and Mathematics at the University of Passau, Germany. Since 2006, he works in the field of timescales and clock algorithms at the Institute of Communication and Navigation (German Aerospace Centre, DLR), Oberpfaffenhofen.

Demetrios Matsakis received his PhD in physics from the University of California at Berkeley. He is Head of the USNO Time Service Department.

ABSTRACT

The GPS system is simulated in three scenarios, so as to estimate how its performance would be improved by more stable ground clocks. One scenario is an approximation to the current system. The second replaces the cesium frequency standards at the monitor sites with masers. The third replaces the masers at the two USNO-controlled monitor sites with atomic fountains. The simplifications exaggerate the differences between the scenarios, and the results suggest that the three scenarios are similar in the timing information as delivered to the user for positioning, but that GPS Time could be more stable with improved clocks. Results are tentative, pending more realistic simulations.

INTRODUCTION

In the beginning, the GPS control segment consisted of 5 monitor stations including one master control station at Schriever AFB. In 2005, the data from 11 additional control stations operated by the National Geospatial-Intelligence Agency (NGA) were integrated to the GPS control segment (Figure 1). In this work, we simulate data from only 11 stations - the original stations plus Washington, DC, Ecuador, Argentina, England, Bahrain, and Australia [1,2].

The monitor stations at Washington DC, USNO and Schriever, AFB are referenced to masers, while all other stations are equipped with HP 5071 Cesium clocks [3, 4]. The paper uses a simplified model of the operational GPS Kalman Filter to investigate by simulation the impact of

improved monitor station clocks on the GPS timing performance.

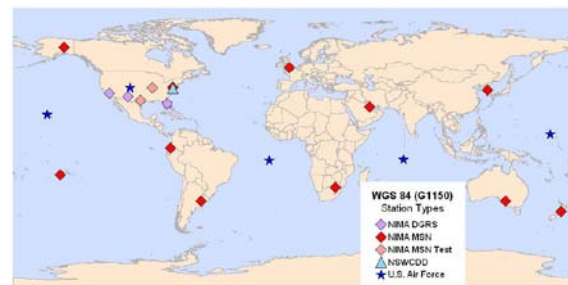


Figure 1: GPS control segment

SIMULATION OF THE GPS WORKFLOW

Using the GPS toolkit software [5], 31 satellites are modeled based on the GPS almanac file of week 531. The satellites are equipped with Rubidium Atomic Frequency Standards (RAFS). Each monitor station observes the time offset, compared to its reference clock, of the satellites in view. The measurements are simulated with a 15-minute spacing, a noise of 0.7 ns (1 sigma), and an elevation angle mask of 20°.

The clock parameters computed by the Kalman Filter are uploaded to each satellite once a day as a broadcast model. In this simulation we assume the update occurs when the satellite is in view over Schriever and the clock broadcast parameters are older than 1 day.

For this work, only clock parameters are solved for. In the operational filter, satellite orbit and other parameters are simultaneously included and the correlations among the full set of parameters would be expected to decrease the precision of the derived solutions. This would most likely decrease the differences we have computed between the clock models.

SIMULATION OF THREE IMPROVED MONITOR STATION CLOCKS AND SATELLITE CLOCKS

Clocks are modeled with a 3-state vector $X(t)$, which is their phase, rate, and drift [6,7]. It is modeled by the stochastic differential equation (SDE)

$$\frac{d}{dt} X(t) = \begin{pmatrix} 0 & 1 & 0 \\ 0 & 0 & 1 \\ 0 & 0 & 0 \end{pmatrix} X(t) + W(t)$$

$$EW(t)W^T(t) = \begin{pmatrix} q_1 & 0 & 0 \\ 0 & q_2 & 0 \\ 0 & 0 & q_3 \end{pmatrix}$$

The three q 's measure the noise contributions from white frequency modulation, random walk frequency modulation, and random run frequency modulation. Neglecting some terms [8], the q 's can be related to the Allan and Hadamard Deviations as:

$$ADEV^2(\tau) = q_1\tau^{-1} + \frac{1}{3}q_2\tau + \frac{1}{20}q_3\tau^3 + \dots$$

$$HDEV^2(\tau) = q_1\tau^{-1} + \frac{1}{6}q_2\tau + \frac{11}{120}q_3\tau^3 + \dots$$

The discrete solution of the SDE, with τ equal to 15 min, is used to simulate the clock types [6,7,8]. Following the assumptions of the Kalman Filter, it can be shown that the process noise matrix Q is a simple function of the q 's and the filter time spacing:

$$\begin{pmatrix} q_1\tau + q_2\frac{1}{3}\tau^3 + q_3\frac{1}{20}\tau^5 & q_2\frac{1}{2}\tau^2 + q_3\frac{1}{8}\tau^4 & q_3\frac{1}{6}\tau^3 \\ q_2\frac{1}{2}\tau^2 + q_3\frac{1}{8}\tau^4 & q_2\tau + q_3\frac{1}{3}\tau^3 & q_3\frac{1}{2}\tau^2 \\ q_3\frac{1}{6}\tau^3 & q_3\frac{1}{2}\tau^2 & q_3\tau \end{pmatrix} = Q(\tau)$$

Three different types of monitor station clocks are simulated: cesium, active hydrogen maser (AHM) and fountain clocks. Their stochastic components (q 's) are specified in table 1, and typical Allan deviations are shown in Figure 2. The values for these q 's should not be taken as authoritative by any means, nor should the associated Allan Deviations be assumed as anything but a rough approximation.

	q_1 WFM	q_2 RWFM	q_3 RRFM
Cesium	2.50e-23	4.44e-37	5e-53
Maser (AHM)	2.8e-26	1.1e-35	4.4e-51
Fountain	4.4e-27	1.1e-37	1.1e-55
RAFS	1.0e-24	1.1e-35	2.8e-46

Table 1: Clock noise models. Printed values are scaled by factor of 900 from the rounded-off values used to generate the time series.

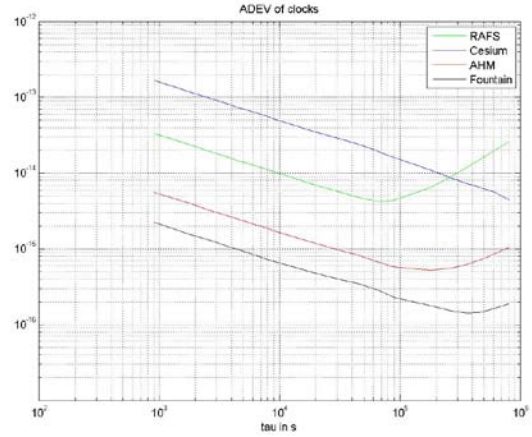


Figure 2: Allan deviation of one individual clock simulation of each modeled type. It assumed that the necessary resources are expended to keep the masers and the atomic fountains within their environmental specifications.

COMPOSITE CLOCK - KALMAN FILTER PROCESSING

The Composite Clock algorithm [7] is applied to process the time offset measurements between the control stations and the satellite clocks and to estimate the satellite and control station clocks with respect to its implicitly defined mean. Due to the fact that N clocks with three states involve $N-1$ measurements, the formal covariance of the solution parameters will grow without bound. This obscures intuitive understanding of the solutions and also can result in problems due to computer limitations in handling large numbers. However, it can be shown [6] that no measured quantity is affected if the Kalman Filter covariance estimates $C(t)$ are reduced as follows:

$$C_{red}(t) = C(t) - H * (H *^T C(t)^{-1} H *)^{-1} H *^T$$

As a test of the programming, we have computed solutions with and without the covariance reduction, and verified that all quantities seen by the user are indeed unchanged.

THREE GROUND SEGMENT SCENARIOS

Table 2 outlines three different ground segment scenarios for the stability of the monitor station clocks.

Model C	Cesium at every station except for Active Hydrogen Masers (AHMs) at Schriever and USNO
Model M	AHMs at every station
Model F	Cesiums at every station except at Schriever and USNO, where USNO will maintain rubidium-based atomic fountains

Table 2: Definition of Scenarios

Model C describes the current situation in GPS whereas Models M and F are possible future scenarios.

PERFORMANCE INDICES 1 AND 2 - THE TIME RELATED USER RANGE ERROR AND THE GPS SATELLITE SYSTEM TIME STABILITY

In order to assess the different scenarios two performance indices are defined which just depend on the satellite clocks and its clock estimates.

The first index measures the accuracy of the clock broadcast models (BM), which are the latest uploads of their three-state Kalman filter estimates. For each satellite k , the broadcast model is updated at least every 24 hours and consists of three parameters used by the users to correct the clock:

$$BM_k(t) = a_0 + a_1(t - t_{upload}) + \frac{1}{2}a_2(t - t_{upload})^2$$

For each value $clk_k(t)$ of clock k at time t , the error in this correction is given by

$$err_k(t) = clk_k(t) - BM_k(t)$$

The RMS of the difference of the corrected clock k to the remaining corrected clocks is calculated at each measurement epoch t :

$$E_k^2(t) = \frac{1}{(31-1)} \sum_{\substack{i=1, \\ i \neq k}}^{31} (err_k(t) - err_i(t))^2$$

The square-rooted average over all satellites defines the performance index 1 (PI1) at time t :

$$PI1(t) = \left\{ \frac{1}{N_{sat}} \sum_{i=1}^{N_{sat}} E_i^2(t) \right\}^{\frac{1}{2}}$$

PI1 is understandable as the average asynchronization of the broadcast model-corrected clocks at time t . It is a measure of the signal-in-space limitations to real-time positioning or synchronization with GPS. In order to allow the clock parameter determinations to mature (become independent of initial assumptions), PI1 (and PI2), are computed excluding the first day's data.

The second performance index, PI2, assesses the stability of GPS Time as computed within the Kalman filter. The GPS satellite time is calculated by

$$sys(t) = \sum_{i=1}^N w_i (clk_i(t) - \hat{x}_i(t))$$

Where the sum is over all system clocks, $x_i(t)$ are the predicted values, and the w_i are the normalized clock weights, given by the inverse covariance of their associated parameters. Assuming the time t is large enough for the parameters to fully mature, PI2 is stationary and given by the Allan Deviation of the system time.

We note that actual GPS Time is stabilized through steering to UTC(USNO). This steering becomes significant on the scale of a few days, and is ignored here. It also follows that the stability of GPS Time itself is only relevant to the extent it minimizes the amount of steering applied to GPS Time. However, GPS Time is intended

for navigational purposes only; users interested in UTC should apply the corrections broadcast in subframe 4 page 18 of the GPS Navigation message to derive UTC(USNO) directly.

EVALUATION OF THREE SCENARIOS

Tables 3 and 4 show PI1 and selected PI2-values for each scenario. The PI1's are averages over the results shown in Figure 3. Figure 4 plots PI2 for each scenario.

Model	PI1 in ps
Model C	500
Model M	434
Model F	433

Table 3: Performance Index 1, RMS of satellite clock differences with broadcast model

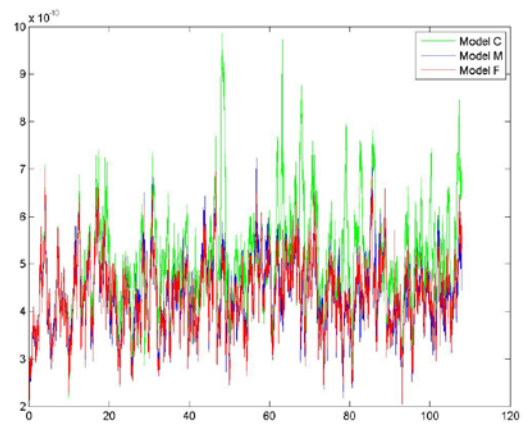


Figure 3: Fifteen-minute contributions to performance index 1 for the three scenarios

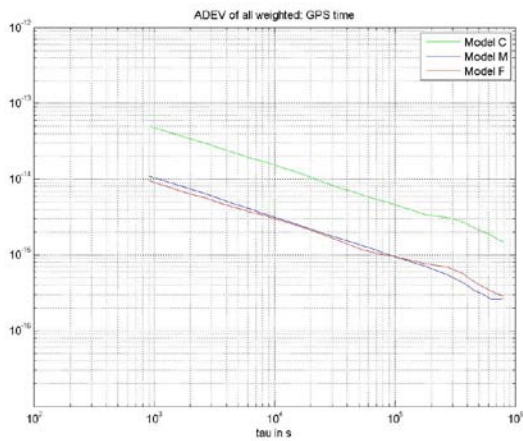


Figure 4: Performance index 2. Weighted average of corrected clocks (GPS Time), for the three scenarios

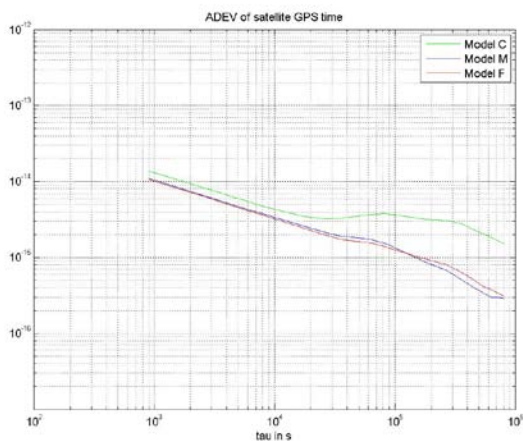


Figure 5. Weighted average of corrected satellite clocks using broadcast corrections This is "PI2" as seen by a user in the field.

Model	PI 2 900s, e-15	PI 2 1 day, e-15
Model C	51	4.9
Model M	11	1.0
Model F	11	1.1

Table 4: Time average of PI2, given the precise clock and models and solution simplifications

Table 3 and figure 3 show very little difference between models C, F, and M in PI1, which is a measure of GPS's real-time signal-in-space performance. This is expected because any improvements in the predictive ability should be masked by the individual satellite clocks' stochastic variations over the 24 hours between uploads.

In contrast, the PI2 values given in Table 4 and Figure 4 show that use of better ground clocks would result in GPS Time being more stable with regards to UTC. Similar results are shown in Figure 5, which is how PI2 would be computed by a world-wide array of receivers that did not have direct access to the GPS ground clocks and could only observe satellite broadcasts. Since the model parameters for atomic fountains result in one fountain being roughly as stable as the rss-stability of an average of five masers, it is also not surprising that in an 11-station solution Models M and F are equivalent and also more stable than Model C. However, as noted above, UTC itself can be more directly inferred from the GPS signals through the broadcast corrections that bring GPS Time to the UTC realization known as UTC(USNO). Therefore the effect of improved PI2 is to decrease the required steering of GPS Time and the uncertainty in the broadcast corrections for UTC(USNO).

CONCLUSIONS

Using a limited set of ground stations and a highly simplified model for the operational GPS Kalman Filter, it has been shown that the real-time positioning ability of GPS is insensitive to the improved ground clocks. In contrast, GPS Time within the Kalman Filter would be more stable if all GPS sites had environmentally-protected masers or the USNO-controlled sites had atomic fountains.

In follow-up work, we intend to incorporate the full array of GPS monitor sites, include the effects of orbital and other parameters, and also to study different algorithms for time extraction, such as filter tuning, parameterization for non-white noise in clocks and observations, and steering to a stable ground reference.

ACKNOWLEDGEMENTS

The authors express their gratitude to Jens Hammesfahr (DLR) for valuable discussions and to Benjamin Harris for invaluable assistance with the GPS Toolkit.

REFERENCES

- [1] <http://www.aero.org/education/primers/gps/elements.html>
- [2] http://www.kowoma.de/en/gps/control_segment.htm
- [3] Mobbs, S. and Hutsell, S. T. "Refining Monitor Station Weighting in the GPS Composite Clock", 29th Annual Precise Time and Time Interval (PTTI), 1997
- [4] D. Manning, "AF/NGA GPS Monitor Station High-Performance Cesium Frequency

Standard Stability 2007/2008: From NGA Kalman Filter Clock Estimates”, 40th Precise Time and Time Interval Meeting (PTTI), 2008

[5] Timothy J. H. Craddock, Richard John Broderick, Colin P. Petersen, and Alex Hu “The GPS Toolkit: Open Source Clock Tools” 40th Precise Time and Time Interval Meeting (PTTI), 2008

[6] K. R. Brown, 1991, "The Theory of GPS Composite Clock" Proc. ION GPS-91 Meeting (Albuquerque, NM, USA) pp 223-41

[7] Galleani, L. “A mathematical model for the atomic clock error” Metrologia, 2003, 40

[8] Zucca, C. and Tavella, P. “The clock model and its relationship with the Allan and related variances” IEEE Transactions on Ultrasonics, Ferroelectrics and Frequency Control, 2005, 52